Kinetic Mechanism of Transcription Initiation by Bacteriophage T7 RNA Polymerase†

Yiping Jia and Smita S. Patel*

Department of Biochemistry, The Ohio State University, 484 West 12th Avenue, Columbus, Ohio 43210

Received December 11, 1996; Revised Manuscript Received February 11, 1997⊗

ABSTRACT: The kinetic mechanism of transcription initiation by bacteriophage T7 RNA polymerase was investigated using transient state kinetic methods. Transcription by bacteriophage T7 RNA polymerase occurs in three stages consisting of initiation, promoter clearance, and elongation. Abortive products, up to 6−8-mer, were synthesized during the initiation phase; the transition from initiation to elongation occurred between the synthesis of 6−8-mer and 11−12-mer, and the processive elongation phase began after the synthesis of 12-mer RNA. Our results show that the synthesis of elongation product from the Φ10 promoter is limited both by the efficiency of initiation and by the frequency at which the polymerase escapes the promoter. Studies with heparin trap suggest that the polymerase maintains contact with the promoter region during multiple turnovers of abortive RNA synthesis; thus, the polymerase does not completely dissociate from the promoter after each event of abortive RNA synthesis. The pre-steady-state kinetics of RNA synthesis indicate that initiation occurs at a rate constant (3.5 s^{-1}) that is about 30 times faster than the steady-state rate constant of RNA synthesis (0.1 s^{-1}). The steady-state rate constant of RNA synthesis is limited largely by the cycling of the RNA polymerase, whereas initiation is limited by the formation of pppGpG, the first RNA product. We show that the synthesis of pppGpG is not limited by steps associated with GTP binding, DNA binding, or the melting of the promoter DNA. Instead, the kinetic results indicate that initiation at the Φ10 promoter is limited either by the first phosphodiester bond formation step or more likely by a conformational change prior to pppGpG formation. Such a conformational change could play a role in proper alignment of the initiating and elongating NTPs for efficient phosphodiester bond formation and in maintaining the fidelity of RNA synthesis.

Transcription initiation plays a major role in regulating gene expression in all organisms. Transcription initiation is a multistep process during which the RNA polymerase locates and binds to a specific promoter sequence, unwinds the dsDNA[1] near the initiation region, and starts RNA synthesis, at a specific position, in a template-dependent manner using rNTPs as substrates. The overall efficiency of initiation and the amount of the final RNA transcript are determined by the efficiency of each of the above steps, which in turn is regulated by the promoter DNA sequence and by accessory proteins. To understand how gene expression can be regulated at the initiation level, one needs to determine which step(s) limit(s) transcription initiation. To this end, it is necessary to understand the kinetic mechanism of initiation which involves dissecting the various steps in the initiation pathway and determining their rate constants.

We have used bacteriophage T7 RNA polymerase as a model system to investigate the detailed mechanism of transcription initiation. T7 RNA polymerase is a 98 kDa single-polypeptide enzyme that contains all the activities necessary for specific initiation, elongation, and termination of RNA synthesis (Chamberlin & Ryan, 1982). Transcription by T7 RNA polymerase is regulated by the sequence of its 17 promoters, which control transcription of all the T7 gene products (Dunn & Studier, 1983), and by T7 lysozyme that acts as a repressor of transcription (Moffatt & Studier, 1987; Ikeda & Bailey, 1992). The strong class III promoters direct efficient synthesis of T7 gene products involved in phage assembly. These promoters are absolutely conserved in DNA sequence from −17 to +6. The weaker class II promoters direct synthesis of gene products involved in DNA metabolism; these promoters share part of the consensus sequence but differ at several positions from the class III promoters.

The crystal structure of T7 RNA polymerase was determined to 3.3 Å resolution (Sousa et al., 1993, 1994). However, the structure was solved in the absence of the DNA; thus, the details of the interaction with the promoter DNA are not known. The overall structure of T7 RNA polymerase is similar to the structure of the Klenow fragment of *Escherichia coli* DNA polymerase I (Ollis et al., 1985) and HIV-1 reverse transcriptase (Kohlsacdt et al., 1992). The RNA polymerase structure is characterized by a deep cleft that must bind the promoter and the template DNA. The so-called palm, finger, and thumb domains of the polymerase define the DNA binding and RNA synthesis catalytic site. Footprinting (Muller et al., 1989) and methylation interference studies (Jorgensen et al., 1991; Maslak et al., 1993) have shown that the polymerase contacts only one side of the DNA helix. Several catalytically important residues that coordinate the essential Mg(II) ions are conserved among

† This research was supported by NIH Grant GM51966 and by an American Cancer Society Junior Faculty Research Award (JFRA 565) to S.S.P.

* Corresponding author. Telephone: 614-292-7763. Fax number: 614-292-6773. E-mail: Patel.85@osu.edu.

⊗ Abstract published in *Advance ACS Abstracts,* April 1, 1997.

[1] Abbreviations: dsDNA, double-stranded DNA; GpG, guanylyl-(3′-5′)guanosine; ITP, inosine 5′-triphosphate; nt, nucleotide; rNTP, ribonucleoside 5′-triphosphate; ssDNA, single-stranded DNA.

S0006-2960(96)03046-2 CCC: $14.00

DNA and RNA polymerases (Osumi-Davis et al., 1992; Woody et al., 1996), and these cluster at the base of the palm domain where the phosphodiester bond formation reaction must occur.

Recent stopped-flow kinetic studies of DNA binding to T7 RNA polymerase have shown that the bimolecular rate of promoter DNA binding is close to diffusion-limited (Jia et al., 1996; Ujvari & Martin, 1996). Moreover, the kinetic studies with the fluorescent 2-aminopurine-modified promoter DNA also suggested that promoter melting was fast and likely occurred simultaneously with DNA binding. Here we investigate the detailed mechanism of transcription initiation with a representative class III, Φ10 promoter. Since transcription initiation is a multistep process, we have used pre-steady-state kinetic methods and kinetic simulation to dissect the intrinsic rate constant of each step during initiation. These studies indicate that the efficiency of steps during both transcription initiation and promoter clearance dictates the amount of the final RNA transcript. Transcription initiation at the Φ10 promoter is not limited by promoter DNA binding or melting. The maximum rate of initiation is limited either by the first phosphodiester bond formation reaction leading to pppGpG formation or by a conformational change preceding that step.

EXPERIMENTAL PROCEDURES

Nucleotide Triphosphates and Other Materials. All rNTPs, GpG, ITP, and heparin were purchased from Sigma Chemical Co. [γ-^{32}P]GTP and [γ-^{32}P]ATP were purchased from ICN Radiochemicals.

Purification of T7 RNA Polymerase. T7 RNA polymerase was purified from *E. coli* strain BL21/pAR1219 (Davanloo *et al*., 1984) kindly provided by Alan Rosenberg and Bill Studier (Biology Department, Brookhaven National Laboratory). The RNA polymerase was purified using three chromatographic columns consisting of SP-Sephadex (polymerase eluted with 200 mM NaCl), CM-Sephadex (eluted with 200 mM NaCl), and DEAE-Sephacel (25−250 mM NaCl gradient, the polymerase eluted around 100 mM NaCl) (Grodberg & Dunn, 1988). The purity of T7 RNA polymerase was checked by SDS−PAGE and was >95% pure as determined by densitometry. The purified enzyme was dialyzed against buffer (20 mM sodium phosphate, pH 7.7, 1 mM Na_3-EDTA, and 1 mM dithiothreitol) containing 100 mM NaCl and 50% (v/v) glycerol, and stored at −70 °C. The enzyme concentration was determined from its molar extinction coefficient at 280 nm of 1.4×10^5 M^{-1} cm^{-1} (King *et al*., 1986).

Synthetic Oligodeoxynucleotides. All oligodeoxynucleotides (Figure 1) were synthesized on an Applied Biosystem 394 DNA synthesizer or on a Millipore nucleic acid synthesis system 899. The DNAs were purified by denaturing polyacrylamide gel electrophoresis (18% polyacrylamide/4.4 M urea). The DNA was visualized by UV shadowing and extracted from the gel by electroelution using an Elutrap apparatus (Schleicher & Schuell).

DNA concentrations were determined by absorbance measurements at 260 nm in TE buffer containing 8 M urea using the following calculated extinction coefficients: 40-mer Φ10 primer, 420 240 M^{-1} cm^{-1}; 40-mer Φ10 template, 451 120 M^{-1} cm^{-1}; 17-mer Φ10 primer, 195 410 M^{-1} cm^{-1}; 60-mer Φ10 primer, 663 090 M^{-1} cm^{-1}; 60-mer Φ10 template, 657 570 M^{-1} cm^{-1}.

The dsDNAs were prepared by annealing complementary ssDNAs. To determine the exact ratio of the complementary ssDNAs, a constant amount of one ssDNA strand (10 μM) was titrated with increasing amounts of the complementary strand (3−17 μM). Duplex DNA formation was monitored by native PAGE (18%). The 1:1 molar ratio of the DNAs was determined after staining the DNAs with Stains-all dye (Sigma).

5′-^{32}P Labeling of GpG. GpG was radiolabeled with [^{32}P]-P_i using [γ-^{32}P]ATP and T4 polynucleotide kinase (GIBCO BRL). 100 μM GpG, [γ-^{32}P]ATP (20 μCi), and 10 units of kinase in 1 × kinase buffer (50 mM Tris-HCl, pH 7.6, 10 mM $MgCl_2$, and 0.1 mM EDTA, pH 8.0) in a total volume of 50 μL were incubated at 37 °C for 1 h; the reaction was stopped by heating the mixture to 75 °C for 20 min. The experiments were carried out by mixing a small amount of [^{32}P]GpG with nonradiolabeled GpG.

Rapid Chemical Quench-Flow Experiments. The pre-steady-state kinetic experiments were conducted using a rapid chemical quench-flow instrument (KinTek Corp., State College PA) designed and built by Johnson (1986). All the experiments were carried out at 25 °C. A typical experiment consisted of loading the enzyme solution (in 50 mM Tris−acetate, 100 mM sodium acetate, 10 mM magnesium acetate, and 5 mM DTT) (Maslak & Martin, 1994) in one syringe, and the [γ-^{32}P]GTP + NTPs (in 50 mM Tris−acetate, 10 mM magnesium acetate, and 5 mM DTT) in a second syringe. The transcription reactions were initiated by mixing the two solutions, and the reactions were stopped after 5 ms to several seconds by mixing with 1 N HCl from a third syringe in the quench-flow apparatus. The quenched reactions were neutralized with 0.25 M Tris base and 1 M NaOH in the presence of chloroform.

Analysis of the Transcription Products. The RNA products were analyzed on a highly cross-linked 23% polyacrylamide/3 M urea gel (the stock consisted of 40% acrylamide/3% BIS). The products were resolved on a Bio-Rad sequencing gel apparatus (0.25 mm comb). Electrophoresis was conducted at 55 °C (110 W) for about 2 h. Small transcription products differing by a single base were separated on the gel. Both the substrate ([γ-^{32}P]GTP) and the product RNAs (correct and incorrect) were quantitated either on a Betascope (Betagen) or on a PhosphorImager instrument (Molecular Dynamics).

Data Analysis. The kinetic data were fit to one of the following equations by a nonlinear least-squares method using KaleidaGraph or SigmaPlot softwares:

$$\text{burst equation: } A(1 - e^{-kt}) + bt + c$$

where A is the burst amplitude, k is the exponential burst rate constant, b is the linear steady-state velocity, and c is the y-intercept.

$$\text{Hill equation: } Vs^n/(K_d + s^n)$$

where V is the maximum velocity, K_d is the apparent equilibrium dissociation constant, s is the substrate concentration, and n is the Hill coefficient.

$$\text{hyperbolic equation: } Vs/(K_d + S)$$

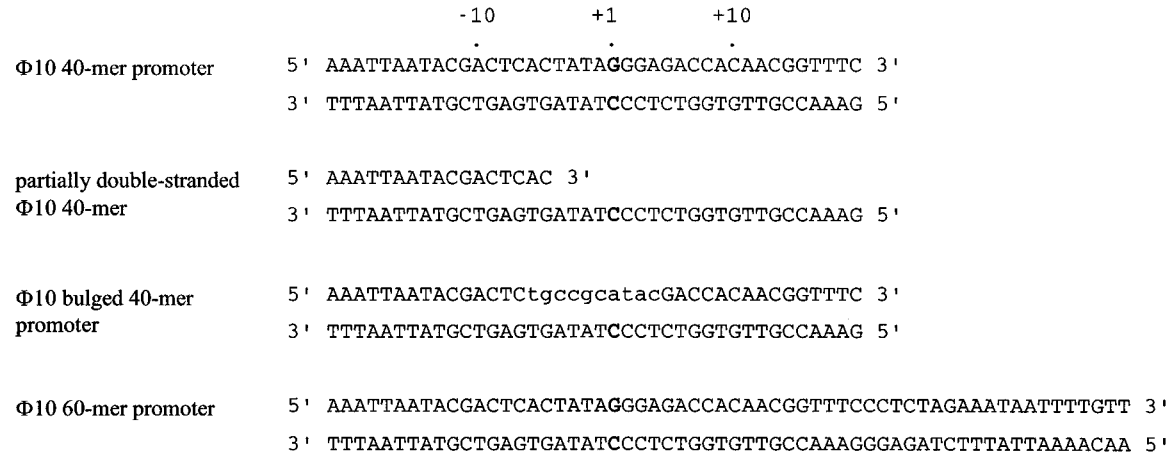

FIGURE 1: Sequences of synthetic promoters for T7 RNA polymerase. The base pairs in boldface are the initiation sites, designated as position +1. The modified sequence of the bulged promoter is in lowercase.

where V is the maximum velocity, s is the substrate concentration, and K_d is the apparent equilibrium dissociation constant.

Kinetic Simulation. Kinetic simulations were performed using the HopKINSIM program (Barshop et al., 1983). The rate constants obtained from the computer-generated fit of the observed kinetics to the above equations were used as initial estimates to arrive at a mechanism during the kinetic simulation process. We arrived at the final mechanism and the rate constants, shown in Scheme 1, from the best global fit to the experimental results shown in Figures 5 and 6. The agreement between the kinetic results and the simulated curves was determined by visual inspection. Even though the rate constants for intermediate RNA formation and dissociation, such as the 3-mer to 6-mer, were not directly measured, the kinetic simulation provided very good estimates of these rate constants because of the constraints due to global fitting.

RESULTS

We investigate here the kinetics of transcription initiation by T7 RNA polymerase to dissect the rate constants of the elementary steps in the initiation pathway. Synthetic promoter DNAs (Martin & Coleman, 1987), 40 bp or 60 bp in length, that contained the natural T7 sequence of the strong Φ10 promoter (from −21 to +19 or +39) were used in all the studies (Figure 1). Since GTP is the initiating nucleotide, transcription reactions were carried out in the presence of [γ-^{32}P]GTP, conditions under which the RNA products would be radiolabeled at the 5′-end. The RNA products were resolved on a high-percentage polyacrylamide/urea gel that separated 2-mer to 19-mer RNAs from each other and from the substrate [γ-^{32}P]GTP. Quantitation of substrate and product on the same gel facilitated normalization of data at each time point and increased the accuracy of the quantitative kinetic measurements.

Transcription Initiation and Elongation at the Φ10 Promoter. To investigate the processivity and the efficiency of RNA synthesis by T7 RNA polymerase during initiation and elongation phases, we have used a longer 60 bp DNA containing the Φ10 promoter sequence and 39 bases of coding region. Transcription reactions were carried out at 25 °C using 15 μM T7 RNA polymerase, 10 μM 60-mer promoter DNA, and 500 μM of four NTPs. High concentrations of polymerase and DNA were used in the experiments to accurately measure RNA synthesis in the first few turnovers. Figure 2A shows the time course of RNA synthesis. Small RNA products, from 2-mer to 7-mer, accumulated during the reaction as abortive products. Beyond 7−8-mer, there was little accumulation of intermediate RNA products, except 11- and 12-mer RNA. Transcription therefore occurred in three stages: During the initiation phase, RNAs 7−8-mer in length were synthesized, but the processive elongation phase began only after the synthesis of 11−12-mer. The RNAs from 8-mer to 12-mer appear to be synthesized in the transition phase between initiation and elongation. Note that besides the correct RNA products, detectable amounts of incorrect RNAs also accumulated during initiation. For example, there are two 3-mer RNA bands and three 4-mer RNA bands. Some of the incorrect RNAs are misincorporation products, and others are oligo-$(rG)_n$ products from promoter slippage. The oligo$(rG)_n$ products, from 2-mer to 4-mer, were identified by comparing to standard RNA products from a reaction containing GTP alone (data not shown). We have included both the correct and the incorrect RNA products in the quantitation of the abortive products.

Figure 2B shows quantitation of the abortive, runoff, and total RNA products as a function of time. The time courses follow linear kinetics with positive intercepts. The slope provided the velocity of RNA synthesis. The positive intercepts are a measure of the [E•D], because the first turnover of RNA synthesis is faster than subsequent turnovers (see below). The slope/[E•D] provided the steady-state rate of RNA synthesis equal to 0.065 ± 0.0025 s^{-1} for abortive RNA products, 0.017 ± 0.0022 s^{-1} for runoff RNA product, and 0.083 ± 0.0042 s^{-1} for total RNA products. The abortive products were synthesized about 3 times faster than the runoff product, indicating that close to 1 out of 4 times the polymerase escapes from cycles of abortive synthesis to synthesize the elongation products.

The following experiment was designed to investigate if multiple turnovers of abortive RNA synthesis occurred with the polymerase still bound to the DNA. To trap free RNA polymerase, we used 5 mg/mL heparin. The effectiveness of heparin as a trap of free polymerase was tested by preincubating 5 μM polymerase and 5 μM 40-mer Φ10 promoter DNA with heparin and initiating the reactions by adding NTPs last. As shown in Figure 3A, transcription was greatly reduced when polymerase was preincubated with

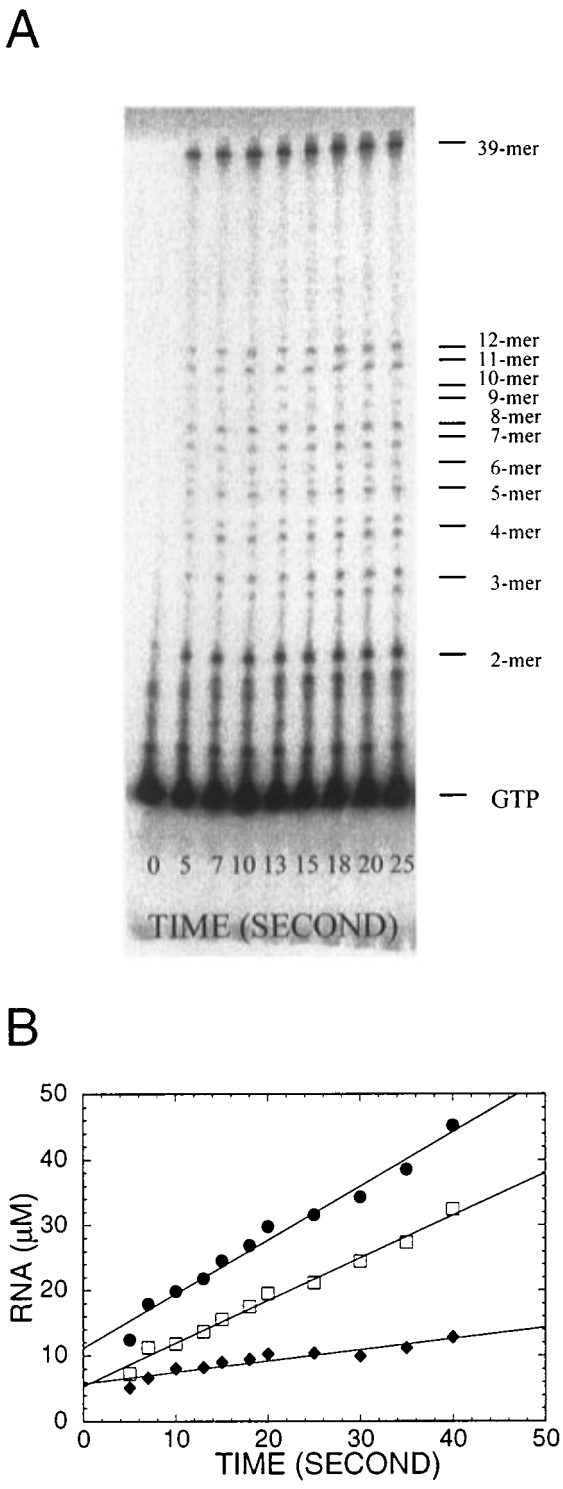

FIGURE 2: Kinetics of RNA synthesis by T7 RNA polymerase at a 60-mer Φ10 promoter DNA. T7 RNA polymerase (15 μM) and 60-mer Φ10 promoter DNA (10 μM) were preincubated, and all four NTPs (500 μM each) + [γ-^{32}P]GTP were added to start the reactions. After time intervals ranging from 5 to 25 s, the reactions were acid-quenched and neutralized, and the RNA products were resolved on a 23% polyacrylamide/3 M urea gel. (Panel A) The Phosphorimager scan of the gel shows the time course of RNA synthesis. (Panel B) The kinetics of abortive RNA products (2-mer to 12-mer) (□), the runoff product (near 39-mer) (◆), and total RNA products (●) fit to straight lines with slopes of 0.65 ± 0.025, 0.17 ± 0.022, and 0.83 ± 0.042 μM·s^{-1} and *y*-intercepts of 5.4 ± 0.56, 5.8 ± 0.51, and 11.2 ± 0.96 μM, respectively.

heparin. In the experiments described below, the final rates were obtained by subtracting the slow rate of RNA synthesis in the presence of heparin.

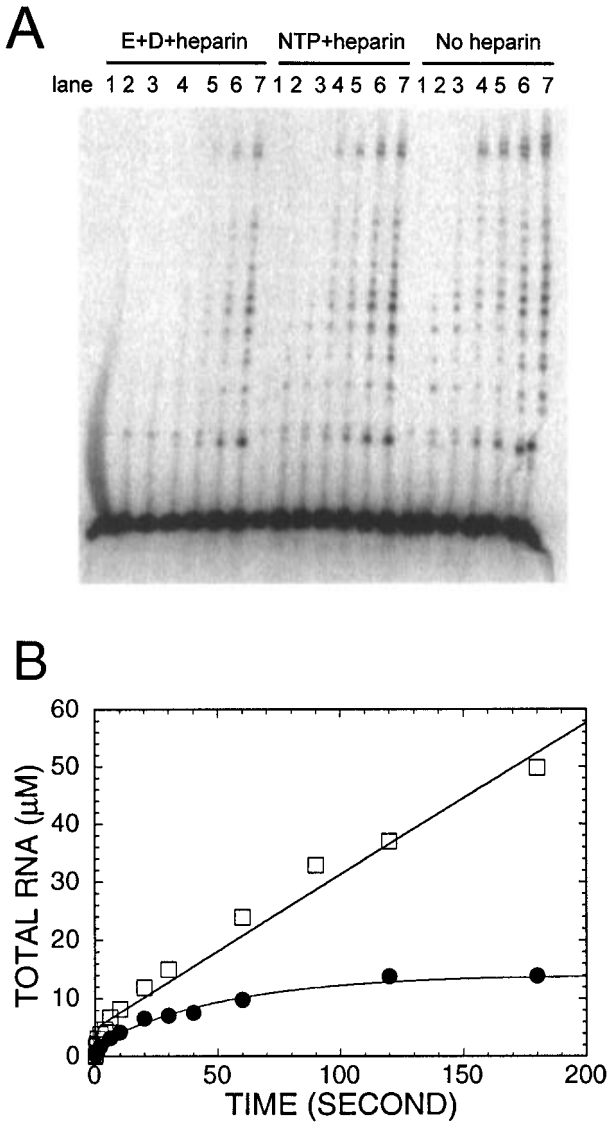

FIGURE 3: Kinetics of RNA synthesis in the presence of heparin as a trap. T7 RNA polymerase (5 μM) and 40-mer Φ10 dsDNA promoter (5 μM) were preincubated, and all 4 NTPs (500 μM) + [γ-^{32}P]GTP were added to start the reactions. The reactions were carried out in the absence or in the presence of heparin (5 mg/mL). The RNA products were resolved on a high-percentage gel, which was analyzed on a Phosphorimager. (Panel A) The Phosphorimager scan of the gel shows the RNA products formed in a control reaction (a), where the polymerase and DNA were preincubated with heparin; in (b), where polymerase and DNA were preincubated and heparin was added with the NTPs; and in (c), where the reactions were performed in the absence of heparin. Lanes 1−7 in each experiment represent reaction times of 0, 0.2, 0.5, 4, 10, 60, and 240 s, respectively. (Panel B) The kinetics of total RNA synthesis in the absence of heparin (□) (reaction c) fit to the burst equation with a burst amplitude of 3.8 ± 0.38 μM, burst rate constant 1.4 ± 0.34 s^{-1}, and steady-state velocity 0.43 ± 0.03 μM·s^{-1}. The kinetics of total RNA synthesis in the presence of heparin (●) (reaction b subtracted from reaction a) show inhibition of RNA synthesis after 4 turnovers of RNA synthesis. The kinetics fit to a sum of two exponential with rate constants 0.91 ± 0.48 s^{-1} and 0.019 ± 0.0023 s^{-1} and amplitudes 2.7 ± 0.57 μM and 12.1 ± 0.54 μM, respectively.

The kinetics of RNA synthesis were measured both in the absence and in the presence of heparin. If RNA polymerase forms a weak complex with the promoter DNA such that it dissociates from the DNA rapidly relative to the rate of initiation, then no synthesis should be observed upon addition of NTPs+heparin. On the other hand, if the polymerase

Scheme 1: Minimal Mechanism of Transcription Initiation by T7 RNA Polymerase

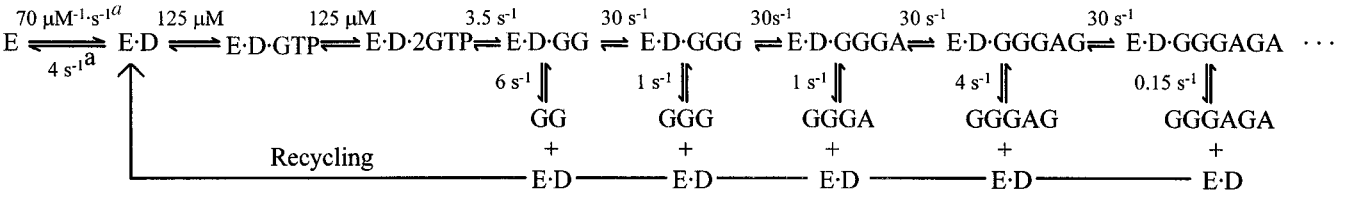

[a] These rate constants were determined previously using stopped-flow methods (Jia et al., 1996).

forms a tight complex, but dissociates from the DNA after each round of abortive RNA synthesis, then only stoichiometric amounts of RNA should be observed. That is, the amount of RNA should be equal to [E·D]. If the polymerase forms a tight complex with the DNA and reinitiates without dissociating from the promoter DNA, then RNA products in excess of [E·D] should be observed.

The results (Figure 3A) show a significant amount of RNA synthesis when heparin was added with the NTPs. The amount of total RNA formed was close to 15 μM, which is about 3 times the [E·D] (5 μM) used in the experiment (Figure 3B). The polymerase therefore had turned over at least 3 times before it was trapped by heparin. Why does the RNA polymerase turn over only 3 times in the presence of heparin? This may be due to two reasons: First, 1 out of 4 times the polymerase escapes the promoter and enters the elongation phase to synthesize the runoff product. If the polymerase dissociates from the DNA after synthesis of the runoff product, this would be one route by which it can get trapped. Second, during each reinitiation event, close to 50% of the polymerase must dissociate from the DNA and get trapped, because the dissociation rate constant of the polymerase from the dsDNA promoter (4 s^{-1}) is close to the initiation rate constant (3.5 s^{-1}; see Scheme 1).

Steady-State and Pre-Steady-State Kinetics of RNA Synthesis during Transcription Initiation. We study here in more detail the pre-steady-state and steady-state kinetics of transcription initiation to determine the step(s) that limit(s), RNA synthesis during transcription initiation. The initiation region of the Φ10 promoter contains the coding sequence (+1)GGGAGACC. In the presence of GTP alone, the polymerase tends to synthesize poly(G) RNA products. Although the analysis of both the steady-state and the pre-steady-state kinetic experiments would have been simpler in the presence of GTP alone, G-ladder synthesis is not a normal initiation event. Thus, we have carried out all our kinetic studies in the presence of GTP and ATP, conditions under which minimal G-ladder synthesis occurred, and 2-mer to 6-mer RNAs were the major reaction products. The synthesis of 2-mer to 6-mer RNA was measured first under steady-state conditions. The RNA polymerase and the 40 bp Φ10 promoter DNA were used in catalytic amounts relative to [GTP] and [ATP]. RNA synthesis under these conditions followed linear kinetics (Figure 4A), and the slope/[E·D] provided a turnover rate constant of 0.11 ± 0.0039 s^{-1}. This turnover rate constant of 2-mer to 6-mer abortive product formation or the steady-state rate is close to the rate constant of abortive RNA synthesis in the presence of all four NTPs (0.065 ± 0.0025 s^{-1}, Figure 2B).

To determine which step limits the steady-state synthesis of abortive RNA products and to determine the slowest step during initiation, we have carried out a detailed pre-steady-state kinetic analysis of RNA synthesis during initiation. The difference between the steady-state and the pre-steady-state experiments is in the experimental design. During steady-state kinetic measurements, one uses catalytic amounts of the enzyme and DNA. In the pre-steady-state experiments, reactions are carried out with higher concentrations of RNA polymerase and promoter DNA such that the ratio of [E·D] to [GTP] is as high as practically possible. This allows accurate measurement of the kinetics of RNA synthesis in the first turnover.

The pre-steady-state kinetic experiments were carried out at 25 °C using a rapid chemical quench-flow apparatus that allowed kinetic measurements in the millisecond time-scale. 30 μM RNA polymerase was preincubated with 20 μM DNA, and the E·D complex was mixed with GTP + [γ-^{32}P]-GTP + ATP to initiate the reactions. The reactions were stopped with HCl, and the RNA products were analyzed on a high-percentage polyacrylamide sequencing gel. Figure 4B shows the gel image of 2-mer to 6-mer RNA synthesis and Figure 4C the kinetics of RNA synthesis. The pre-steady-state kinetics of transcription initiation were biphasic (burst kinetics) (Johnson, 1992). The fast phase or the burst phase at 3.2 ± 0.42 s^{-1} (at 500 μM GTP and 600 μM ATP) represents the rate of RNA synthesis in the first turnover, and the linear phase describes the kinetics of multiple turnovers. The observation of burst kinetics indicates that the steady-state rate constant of RNA synthesis (0.25 s^{-1}) is limited by a step that occurs after initiation. The burst rate constant is about 30 times faster than the steady-state turnover rate constant, and it is a measure of the efficiency of transcription initiation, and the burst amplitude (15.0 ± 0.74 μM) provides the active [E·D].

Maximum Rate of Transcription Initiation at the Φ10 Promoter. To determine the maximum rate of transcription initiation at the Φ10 promoter and the apparent K_d of GTP, the above pre-steady-state kinetics of transcription initiation were measured at increasing [GTP]. Since the kinetics of RNA synthesis at 600 μM or 1 mM ATP were identical (Figure 4C), [ATP] at 600 μM was used in all experiments. Figure 5A shows the [GTP] dependence of the pre-steady-state kinetics. The initiation rate constants at various [GTP] were determined from the initial slopes of the burst phase, and these were plotted against [GTP] (Figure 5B). The initial rate constant increased with [GTP] before saturation. The [GTP] dependence did not fit to the hyperbolic equation, which describes binding of one GTP to the E·D complex. The data fit to the Hill equation with a Hill coefficient of 2.0, which is consistent with formation of pppGpG from reaction between two GTPs. The present data do not allow us to dissect the individual K_d values of the two GTPs but provide an average K_d of 200 μM (square root of the K_d obtained from the Hill plot) and the maximum rate of initiation equal to 30 μM·s^{-1}.

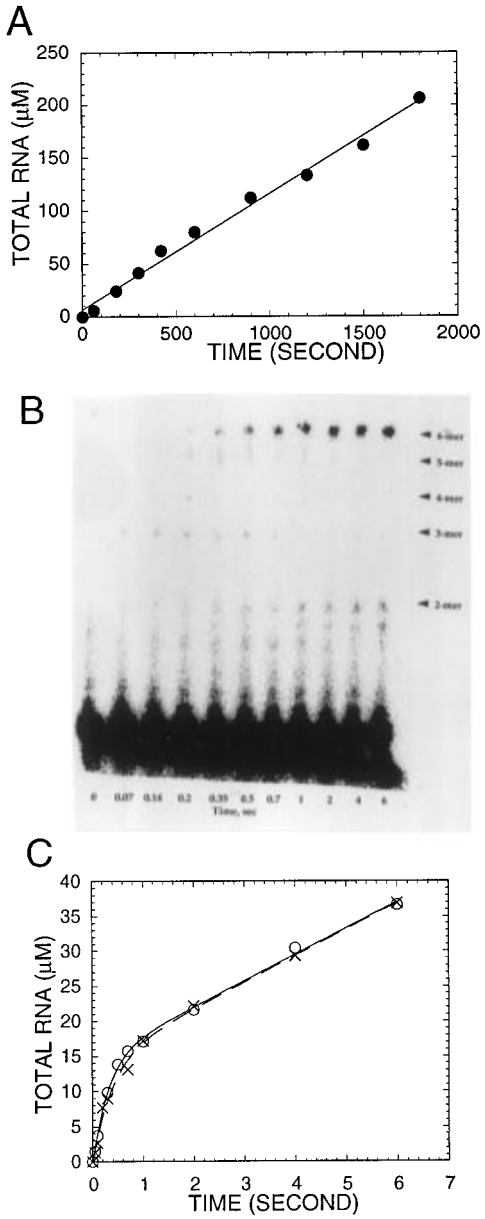

FIGURE 4: Steady-state and pre-steady-state kinetics of transcription initiation at the Φ10 40-mer promoter. (Panel A) The steady-state kinetics of abortive RNA synthesis during initiation were measured at 25 °C using 1 μM T7 RNA polymerase, 1 μM 40-mer Φ10 promoter, 500 μM GTP, [γ-^{32}P]GTP, and 600 μM ATP. After time intervals ranging from 1.0 to 30 min, reactions were acid-quenched, and the resulting RNA products were resolved on a 23% polyacrylamide/3 M urea gel and quantitated on the Betascope imager (Betagen). The time course of total RNA synthesis (●) fit to a straight line with slope of 0.11 ± 0.0039 μM·s^{-1}, which divided by an [E·D] of 1 μM provided a turnover rate constant of 0.11 s^{-1}. (Panel B) The pre-steady-state kinetics of abortive RNA synthesis were measured at 25 °C in a rapid chemical quench-flow instrument. T7 RNA polymerase (30 μM) was preincubated with the 40-mer Φ10 promoter (20 μM) and mixed with GTP (500 μM), [γ-^{32}P]-GTP, and ATP (600 μM) as described under Experimental Procedures. The RNA products were resolved on a 23% polyacrylamide/3 M urea gel, and the Betascope image of the gel shows the time course of RNA synthesis from 2-mer to 6-mer. (Panel C) The pre-steady-state kinetics of RNA synthesis were measured as described in panel B. Total RNA products are plotted versus time for the reaction at 600 μM ATP (○) or 1 mM ATP (×). The solid lines are fit to the burst equation with burst amplitudes (15.0 ± 0.74 and 14.4 ± 1.23 μM), the exponential burst rate constants (3.2 ± 0.42 and 2.6 ± 0.54 s^{-1}), and the linear steady-state rate velocities (3.8 ± 0.17 and 3.8 ± 0.29 μM·s^{-1}) at 600 μM and 1 mM ATP, respectively.

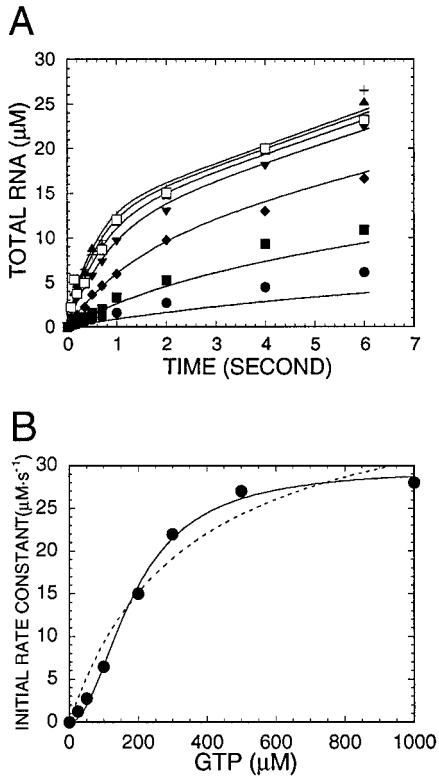

FIGURE 5: [GTP] dependence of the pre-steady-state kinetics of transcription initiation. The pre-steady-state kinetics of abortive RNA synthesis were measured at 25 °C at increasing [GTP] and constant [ATP] in a rapid quench-flow instrument. The 40-mer Φ10 promoter (20 μM) and T7 RNA polymerase (30 μM) were mixed with GTP (25−1000 μM), [γ-^{32}P]GTP, and ATP (600 μM). After time intervals ranging from 0.07 s to several seconds, the reactions were acid-quenched, and the RNA products were analyzed as described under Experimental Procedures. (Panel A) Total RNA products (2-mer to 6-mer) are plotted versus time. Each kinetic trace was obtained at different [GTP]: 25 μM (●), 50 μM (■), 100 μM (◆), 200 μM (▼), 300 μM (+), 500 μM (▲) and 1000 μM (□). The solid lines are simulated kinetic curves generated using the HopKINSIM program with the mechanism and kinetic rate constants shown in Scheme 1. (Panel B) The initial velocities (slope of the burst phase) of the reaction at each [GTP] were determined and plotted versus [GTP]. The solid line is the fit of the data to the Hill equation with a Hill coefficient of 2.0, an average K_d of GTPs equal to 200 μM, and the maximum velocity of RNA synthesis equal to 29.7 μM·s^{-1}. The dotted line shows the fit to the hyperbolic equation with a maximum velocity of 40.8 μM·s^{-1} and the K_d of GTP equal to 340 μM.

Transcription Initiation Is Limited by 2-mer RNA Synthesis. In the above pre-steady-state experiments, we have measured the kinetics of total RNA products, that is, the sum of 2-mer to 6-mer RNAs as a function of time. To determine which RNA synthesis step limits initiation, we have analyzed the kinetics of individual RNA product synthesis. Figure 6A shows quantitation of the individual RNA products, 2-mer to 6-mer, as a function of time. Figure 6B shows the data at shorter reaction time, depicting more clearly the kinetics of RNA synthesis in the first turnover. If each of the RNAs from 2-mer to 6-mer were made at the same rate, then the intermediate RNAs should appear and disappear at uniform intervals. The single-turnover kinetics of 2-mer to 6-mer formation, however, did not fit to a uniform rate of RNA synthesis. In fact, the results show very little accumulation of intermediate RNAs from 2-mer to 5-mer during the first turnover. This indicates that polymerization is limited largely by the first step, that is, formation of 2-mer RNA.

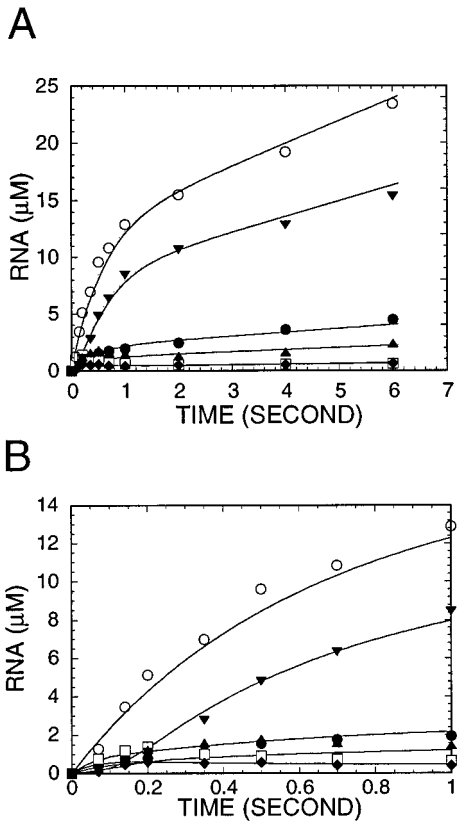

FIGURE 6: Pre-steady-state kinetics of 2-mer to 6-mer RNA product formation during initiation. The kinetics of 2-mer to 6-mer RNA formation in the pre-steady-state experiment described in Figure 5 at 500 μM GTP and 600 μM ATP are shown. Panels A and B show the kinetics of individual RNA synthesis at different time-scales: pppGpG (●), pppGpGpG (□), pppGpGpGpA (◆), pppGpGpGpApG (▲), pppGpGpGpApGpA (▼), and total RNA (○). The solid lines are simulated curves generated using the HopKINSIM program and with the mechanism and the rate constants shown in Scheme 1.

Kinetics of Transcription Initiation Using GpG as the Initiating Nucleotide. To confirm that GpG synthesis from reaction between two GTPs was slower than subsequent bond formation steps, the pre-steady-state kinetics of initiation were measured using GpG as the initiating nucleotide. Use of GpG as the initiating substrate should circumvent the first phosphodiester bond formation step between two GTPs. The 2-mer GpG was labeled at 5′-end with [^{32}P]phosphate. Transcription reactions were carried out using ITP in place of GTP (Martin & Coleman, 1989) to avoid competition with GpG for the initiating position. The kinetics of total RNA synthesis with [^{32}P]GpG + ITP + ATP are shown in Figure 7. Synthesis of RNA products occurred with burst kinetics. The burst rate constant with GpG as the initiating nucleotide was 10.8 ± 1.4 s^{-1}, 3−4 times faster than the burst rate constant with GTP. Note that the steady-state rate of 3-mer to 6-mer RNA synthesis is also faster with GpG versus GTP as the initiating nucleotide. Since the steady-state represents RNA dissociation or polymerase recycling, these steps must be accelerated in the GpG + ITP + ATP reaction.

Promoter DNA Binding Does Not Limit 2-mer RNA Synthesis. All the elementary steps, from DNA binding to the formation of the first phosphodiester bond between two GTPs are possible candidates for the rate-limiting step during initiation. The pre-steady-state kinetics of initiation were measured under the conditions where the polymerase was not preincubated with the DNA to determine if steps

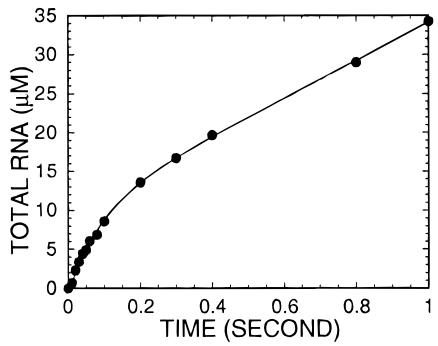

FIGURE 7: Pre-steady-state kinetics of RNA synthesis with GpG as the initiating nucleotide. The pre-steady-state kinetics of RNA synthesis were measured at 25 °C by preincubating T7 RNA polymerase (30 μM) with 40-mer Φ10 promoter (20 μM), and initiating the reactions by mixing it with 200 μM GpG, [^{32}P]GpG, 600 μM ATP, and 500 μM ITP in a rapid chemical quench-flow apparatus. RNA products were analyzed as described under Experimental Procedures. The solid line is the fit of the pre-steady-state kinetics of total RNA synthesis (3-mer to 6-mer) to the burst equation with a burst rate constant of 10.8 ± 1.4 s^{-1} and the steady-state velocity of 24 ± 0.96 μM·s^{-1}.

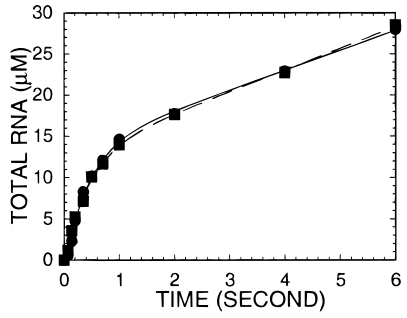

FIGURE 8: Kinetics of transcription initiation with a preincubated or a non-preincubated mixture of T7 RNA polymerase and 40-mer Φ10 dsDNA promoter. T7 RNA polymerase (30 μM) and 40-mer Φ10 promoter DNA (20 μM) were preincubated and mixed with [γ-^{32}P]GTP, GTP (500 μM), and ATP (600 μM) (■) to start the reaction. In a separate reaction, RNA polymerase was mixed with the NTPs+DNA at the start of the reaction (●). Both reactions were acid-quenched, and the RNA products were analyzed as described under Experimental Procedures. The observed pre-steady-state kinetics of RNA synthesis were identical in the two experiments, and the solid lines show the fit to the burst equation with nearly the same burst rate constant (2.3 ± 0.33 s^{-1}) and the steady-state velocity (2.4 ± 0.22 μM·s^{-1}).

associated with DNA binding could limit initiation. The kinetics of initiation were measured under two experimental conditions: one in which the polymerase was preincubated with the DNA, and the other in which the polymerase was mixed with DNA+GTP+ATP at the start of the reaction. The observed kinetics (Figure 8) were identical under the two conditions, indicating that DNA binding or associated steps do not limit the rate of transcription initiation. Pre-incubating the polymerase with GTP and initiating the reaction by adding DNA last did not affect the initiation kinetics (data not shown). This indicates either that GTP does not bind to the polymerase in the absence of the DNA or that if it does, preincubating GTP with the polymerase does not affect the initiation kinetics. The above experiments suggest that the step that limits synthesis of pppGpG during initiation lies between DNA binding and the first phosphodiester chemical bond formation.

The Rate of Transcription Initiation at the Partially dsDNA Promoter Is the Same as the Fully dsDNA Promoter. To

determine if promoter melting limits pppGpG formation, experiments were carried out using a partially dsDNA promoter that was duplex in the promoter recognition region (−21 to −4) and single-stranded in the coding region (from −4 onward in the template strand) (Figure 1). Previous results in the literature have shown that the region −5 to +3 becomes sensitive to single-stranded DNA endonuclease (Strothkamp et al., 1980; Osterman & Coleman, 1981), implying that this region melts during open complex formation. The partially dsDNA promoter therefore should mimic a preformed open promoter. If promoter melting is the slow step that limits initiation, then the burst rate constant should be much faster with the partially dsDNA promoter. The pre-steady-state kinetics of RNA synthesis at the partially dsDNA promoter were compared to those at the fully dsDNA promoter. As shown in Figure 9, transcription initiation at the partially dsDNA promoter occurred with burst kinetics, and the burst rate constant (2.0 ± 0.22 s^{-1}) was nearly the same as with the fully dsDNA promoter (2.7 ± 0.44 s^{-1}). The efficiency and processivity of RNA synthesis (2-mer to 6-mer) at the partially dsDNA and the fully duplex promoter were about the same. The burst amplitude that measures the amount of [E·D] was slightly different with the partially dsDNA versus the fully dsDNA promoters (14.4 ± 0.75 versus 9.2 ± 0.63 μM), and the steady-state rates of RNA synthesis for the two promoters were also different (0.65 ± 0.17 versus 2.6 ± 0.15 μM·s^{-1}). Since the steady-state rate is limited by RNA dissociation or the cycling of the RNA polymerase, the lower steady-state rate suggests that either the ternary complex E·D·RNA is more stable with the partially dsDNA promoter or the polymerase is slower at reinitiating synthesis at the partially dsDNA promoter.

The above experiment was also carried out using a synthetic bulged-DNA promoter, in which the −6 to +4 region of the primer strand was designed to be noncomplementary to the template strand (Figure 1). Transcription initiation from the bulged promoter showed the same burst kinetics under pre-steady-state conditions. The burst rate constant (2.1 ± 0.19 s^{-1}) was comparable to that of the fully dsDNA promoter (2.7 ± 0.44 s^{-1}) (data not shown). These results are in agreement with our conclusion that DNA melting does not limit synthesis of the 2-mer RNA. By elimination, the possible steps that could limit initiation include GTP binding, a conformational change prior to 2-mer formation, or the chemical bond formation between two GTPs may be a slow step. Our results show that the maximum rate of pppGpG formation is not limited by GTP binding because the initiation rate constant saturated at high [GTP] (Figure 5B). Thus, it appears that the chemistry of pppGpG formation or a conformational change prior to pppGpG formation limits transcription initiation at the Φ10 promoter.

Kinetic Simulation. The observed pre-steady-state kinetics of RNA synthesis during initiation shown above in Figures 5 and 6 were simulated to obtain better estimates of the intrinsic rate constants of the elementary steps. Simulated kinetic curves were generated using the computer program HopKINSIM. The minimal mechanism shown in Scheme 1 predicted quite accurately the observed [GTP] dependence kinetics and the kinetics of individual RNA product synthesis (solid lines in Figures 5 and 6). Best fits to experimental data were obtained with a GTP K_d of 125 μM rather than the measured value of 200 μM. Although it is likely that

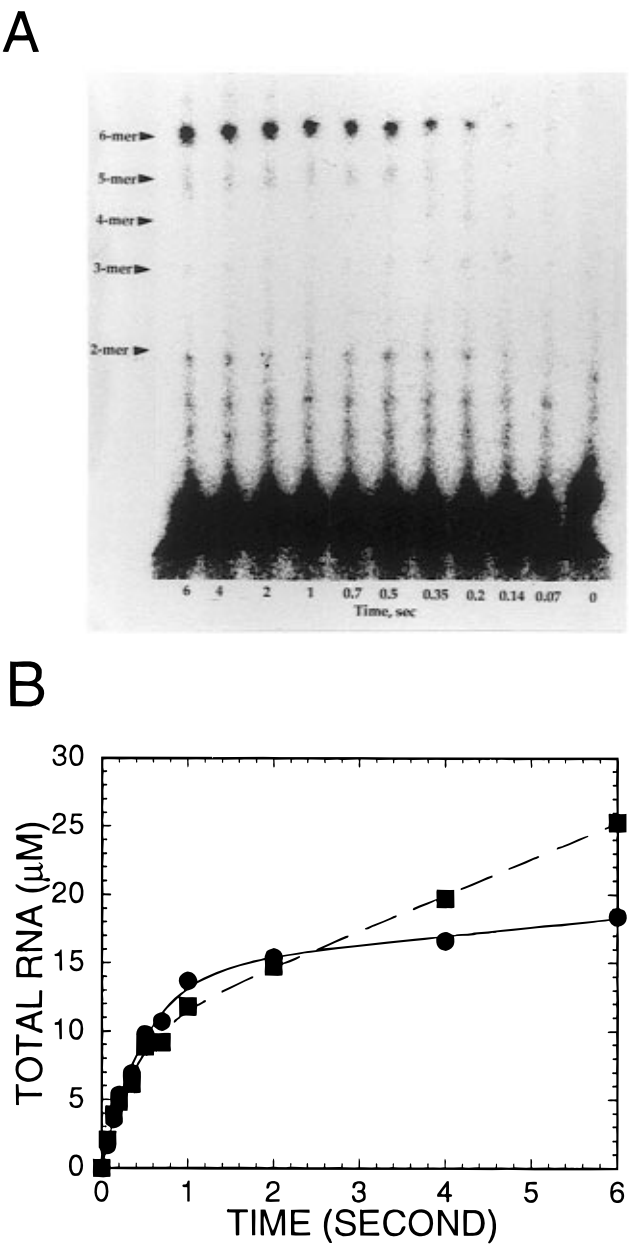

FIGURE 9: Kinetics of transcription initiation at the partially double-stranded Φ10 DNA promoter. The pre-steady-state kinetics of RNA synthesis at a partially double-stranded 40-mer Φ10 promoter are compared to those at the fully dsDNA promoter. A preincubated solution of T7 RNA polymerase (30 μM) and DNA (20 μM) was mixed with 500 μM GTP, [γ-^{32}P]GTP, and 600 μM ATP at 25 °C. The reactions were acid-quenched, and the RNA products were analyzed as described under Experimental Procedures. (Panel A) The Betascope image of the gel shows the time course of RNA synthesis (2-mer to 6-mer) at the partially ds Φ10 DNA. (Panel B) The kinetics of total RNA synthesis at the partially dsDNA promoter (●) and the fully dsDNA promoter (■) are compared. The pre-steady-state kinetics of RNA synthesis at the partially dsDNA promoter fit to the burst equation with a burst rate constant of 2.0 ± 0.22 s^{-1}, burst amplitude of 14.4 ± 0.75 μM, and the steady-state velocity of 0.65 ± 0.17 μM·s^{-1}. The kinetics at the fully dsDNA promoter fit to a burst rate constant of 2.7 ± 0.44 s^{-1}, burst amplitude of 9.2 ± 0.63 μM, and steady-state velocity of 2.6 ± 0.15 μM·s^{-1}.

the two GTPs will have different K_ds; for simplicity we have simulated the kinetics assuming the same K_d for both GTPs. Similarly, the simulated curves fit better to the data with the intrinsic rate constant of pppGpG formation equal to 3.5 s^{-1}. It is clear that polymerase recycling or 6-mer RNA

dissociation is slow and limits the overall rate of RNA synthesis at steady-state. The individual RNA formation kinetics (Figure 6) fit best to pppGpG formation being the slowest step and subsequent steps occurring at a rate constant of 30 s^{-1}. The rate constants for the synthesis and dissociation of intermediate RNAs were not directly measured, and need to be refined; however, the strict constraints of global fit provide reasonable confidence in those rate constants.

DISCUSSION

We investigate here the kinetic mechanism of RNA synthesis by T7 RNA polymerase using transient state kinetic methods. This study provides a minimal mechanism of transcription initiation at a strong Φ10 promoter DNA (Scheme 1). The derived mechanism is likely to be general and applicable to other promoters as well, except the intrinsic rate constants will change depending on the promoter. It will be important to measure these intrinsic rate constants at different promoters if one wishes to understand the kinetic basis of transcription regulation at the level of initiation.

The RNA polymerase catalyzes transcription in three stages consisting of initiation, promoter clearance, and elongation. During initiation, the polymerase is bound stably to the promoter DNA, and RNAs from 2-mer to 6−8-mer are synthesized from a specific initiation region. RNA synthesis is less processive during initiation, and small RNAs dissociate and accumulate during the reaction as abortive products. The kinetic experiments showed that only 1 out of 4 times the polymerase escapes the initiation phase and enters the elongation phase, where RNA synthesis is both processive and efficient. Synthesis of full-length RNA products is therefore dictated by the efficiency of initiation and the frequency of polymerase escape from the promoter.

Abortive RNA products are not formed after the RNAs reach a length of about 12 nts. Up to that point, the frequency of abortive RNA synthesis does not depend on the length of the RNA. That is, we do not observe a gradual decrease in the amount of abortive products with increasing RNA length. It is clear, however, that when the RNA is >12 nt long, synthesis becomes processive. This implies that a specific change occurs in the RNA polymerase after synthesis of 6−8-mer RNA, and this change is complete after the synthesis of 12-mer RNA, at which point the polymerase enters the elongation phase. Such a change has been proposed by a number of investigators, but little is known of the associated structural changes in the E·D complex during such an isomerization. One study in the literature has shown that there is a change in the proteolytic pattern of the RNA polymerase after it enters the elongation phase (Sousa et al., 1992). Another study has shown that the newly synthesized RNA leaves the polymerase active site when it is close to 10−13 nts in length (Tyagarajan et al., 1991). Thus, the isomerization step may represent binding of the newly synthesized RNA into an RNA binding site, which may occur after the RNA reaches a length of 6−8-mer, and the change may be completed after the RNA is about 12-mer in length.

Since the rate of RNA synthesis in the first turnover is faster than the rate in subsequent turnovers, the steady-state rate constant measures the kinetics of a step that occurs after initiation. This step is either RNA dissociation or polymerase cycling, both of which allow reinitiation after an abortive event. We argue that it is unlikely that the dissociation of RNA from the E·D·RNA ternary complex is a slow step because if this were the case then RNA synthesis should have been processive during initiation. It is more likely that RNA dissociation is fast but the cycling of the polymerase or the reinitiation event is the slow step that limits multiple turnover of abortive RNA synthesis. Experiments with heparin trap have shown that the polymerase can cycle, at least 3 times, and synthesize abortive RNA products without fully dissociating from the promoter DNA. Thus, the RNA polymerase maintains contact with the promoter region during RNA synthesis in the initiation phase. This is in agreement with a recent report where polymerase was shown to catalyze multiple rounds of abortive product synthesis at the supercoiled and the partially dsDNA promoters in the presence of a trap (Diaz et al., 1996). We did not observe the polymerase turning over as many times at the dsDNA promoter, most likely because the E·D complex is less stable at the dsDNA promoter relative to the supercoiled and partially dsDNA promoters (Jia et al., 1996; Ujvari & Martin, 1996).

The maximum rate of initiation was not limited by DNA binding or steps associated with DNA binding such as melting of the promoter DNA. These conclusions are supported by several results: First, the initiation rate constant was unchanged whether the polymerase was preincubated or not preincubated with the DNA prior to transcription. We assume that preincubation of the promoter DNA with the RNA polymerase allows sufficient time for promoter melting. Second, the initiation rates were the same for the fully dsDNA and the partially dsDNA or the bulged dsDNA promoters. Again, the assumption is that the partially dsDNA mimics melted DNA. Third, recent stopped-flow studies of DNA binding with 2-aminopurine-containing promoter DNAs have suggested that promoter melting is fast relative to the rate of initiation (Jia et al., 1996; Ujvari & Martin, 1996).

Detailed analysis of the kinetics of the individual RNA product formation (from 2-mer to 6-mer) showed that transcription at the Φ10 promoter was limited by 2-mer RNA synthesis. The kinetics of RNA synthesis suggested that the 3-mer RNA was formed at a faster rate than the 2-mer RNA; therefore, once the first phosphodiester bond is formed, subsequent bond formation reactions are relatively fast. What limits the formation of 2-mer RNA during initiation? Our results indicate that 2-mer RNA synthesis is limited by a step between DNA binding and the phosphodiester bond formation step between two GTPs. Although it needs to be shown, but as with T7 DNA polymerase (Patel et al., 1991) and HIV-1 reverse transcriptase (Kati et al., 1992), it is unlikely that the chemical step itself is rate limiting. The steps that could limit pppGpG formation include binding of initiating and elongating GTPs or a conformational change prior to pppGpG formation. Since the initiation rate constant (as measured by the pre-steady-state burst rate) saturated at high [GTP], pppGpG formation is very likely limited by a conformational change that occurs prior to chemistry, possibly a conformational change that is sensitive to proper base-pairing and that brings the two GTPs in proper alignment for catalysis.

REFERENCES

Barshop, B. A., Wrenn, R. F., & Frieden, C. (1983) *Anal. Biochem. 130, 134*−145.

Chamberlin, M. J., & Ryan, T. (1982) *Enzyme(s) (3rd Ed.) 15*, 87−108.

Davanloo, P., Rosenberg, A. H., Dunn, J. J., & Studier, F. W. (1984) *Proc. Natl. Acad. Sci. USA 81, 2035*−2039.

Diaz, G. A., Rong, M., McAllister, W. T., & Durbin, R. K. (1996) *Biochemistry 35, 10837*−10843.

Dunn, J. J., & Studier, F. W. (1983) *J. Mol. Biol. 166, 477*−535.

Grodberg, J., & Dunn, J. J. (1988) *J. Bacteriol. 170, 1245*−1253.

Ikeda, R. A., & Bailey, P. A. (1992) *J. Biol. Chem. 267, 20153*−20158.

Jia, Y., Kumar, A., & Patel, S. S. (1996) *J. Biol. Chem. 271, 30451*−30458.

Johnson, K. A. (1986) *Methods Enzymol. 134, 677*−705.

Johnson, K. A. (1992) in *Enzyme (3rd Ed.) 20*, 1−61.

Jorgensen, E. D., Durbin, R. K., Risman, S. S., & McAllister, W. T. (1991) *J. Biol. Chem. 266, 645*−651.

Kati, W. M., Johnson, K. A., Jerva, L. F., & Anderson, K. S. (1992) *J. Biol. Chem. 267, 25988*−25997.

King, G. C., Martin, C. T., Pham, T. T., & Coleman, J. E. (1986) *Biochemistry 25, 36*−40.

Kohlsacdt, L. A., Wang, J., Friedman, J., Rice, P. A., & Steitz, T. A. (1992) *Science 258, 1783*−1790.

Martin, C. T., & Coleman, J. E. (1987) *Biochemistry 26, 2690*−2696.

Martin, C. T., & Coleman, J. E. (1989) *Biochemistry 28, 2760*−2762.

Maslak, M., & Martin, C. T. (1994) *Biochemistry 33, 6918*−6924.

Maslak, M., Jaworski, M. D., & Martin, C. T. (1993) *Biochemistry 32, 4270*−4274.

Moffatt, B. A., & Studier, F. W. (1987) *Cell 49, 221*−227.

Muller, D. K., Martin, C. T., & Coleman, J. E. (1989) *Biochemistry 28, 3306*−3313.

Ollis, D. L., Brick, P., & Steitz, T. A. (1985) *Nature 313, 765*−769.

Osterman, H. L., & Coleman, J. E. (1981) *Biochemistry 20, 4884*−4892.

Osumi-Davis, P. A., de Aguilera, M. C., Woody, R. W., & Woody, A.-Y. M. (1992) *J. Mol. Biol. 226, 37*−45.

Patel, S. S., Wong, I., & Johnson, K. A. (1991) *Biochemistry 30, 511*−525.

Sousa, R., Patra, D., & Lafer, E. M. (1992) *J. Mol. Biol. 224, 319*−334.

Sousa, R., Chung, Y. J., Rose, J. P., & Wang, B. C. (1993) *Nature 364, 593*−599.

Sousa, R., Rose, J. P., & Wang, B. C. (1994) *J. Mol. Biol. 244, 6*−12.

Strothkamp, R. E., Oakley, J. L., & Coleman, J. E. (1980) *Biochemistry 19, 1074*−1080.

Tyagarajan, K., Monforte, J. A., & Hearst, J. E. (1991) *Biochemistry 30, 10920*−10924.

Ujvari, A., & Martin, C. T. (1996) *Biochemistry* 35, 14574−14582.

Woody, A.-Y. M., Eaton, S. S., Osumi-Davis, P. A., & Woody, R. W. (1996) *Biochemistry 35, 144*−152.

BI9630467